



# Effect of latrunculin-A on morphology and actin-associated adhesions of cultured human trabecular meshwork cells

Suping Cai,<sup>1</sup> Xuyang Liu,<sup>1</sup> Adrian Glasser,<sup>1</sup> Tova Volberg,<sup>2</sup> Mark Filla,<sup>1</sup> Benjamin Geiger,<sup>2</sup> Jon R. Polansky,<sup>3</sup> Paul L. Kaufman<sup>1</sup>

Departments of <sup>1</sup>Ophthalmology & Visual Sciences, University of Wisconsin, Madison, WI; <sup>2</sup>Molecular Cell Biology, Weizmann Institute of Science, Rehovot, Israel; <sup>3</sup>Ophthalmology, University of California, San Francisco, CA

**Purpose:** Determine the effects of the actin cytoskeleton disrupting compound latrunculin-A (LAT-A) on morphology, cytoskeleton, and cellular adhesions of cultured human trabecular meshwork (HTM) cells.

**Methods:** HTM cells were cultured to high confluence with endothelial-like morphology and treated with LAT-A at different doses and duration. Topography of living cells was evaluated by videomicroscopy. Distribution and organization of the actin-based cytoskeleton, vinculin- and paxillin-containing focal contacts, and  $\beta$ -catenin-rich intercellular adhesions were determined by immunofluorescence and digital microscopy.

**Results:** LAT-A induced pronounced but highly reversible rounding of HTM cells, intercellular separation, and disruption of actin filaments.  $\beta$ -catenin-rich intercellular adheren junctions were particularly sensitive to LAT-A. Vinculin- and paxillin-containing focal contacts were only partially affected and appeared to be more resistant to the drug than the intercellular interactions.

**Conclusions:** The increase in outflow facility in the living primate eye induced by LAT-A may be due to the disorganization and disruption of the actin cytoskeleton and its associated cellular adhesions in the trabecular meshwork.

Pharmacologically induced deterioration of the cytoplasmic microfilament system leads to alterations in the submembrane junctional plaque and consequent weakening of cell-cell and cell-extracellular matrix (ECM) adhesions in several cell types, including human trabecular meshwork (HTM) cells [1-3]. Cytochalasins B and D, EDTA and EGTA, epinephrine, and H-7 are believed to exert their outflow facility increasing effects by these mechanisms [3-7]. LAT-A, a macrolide derived from the marine sponge *Latrunculia magnifica*, is a specific actin disrupting agent that disassembles actin filaments by sequestering monomeric actin [8,9]. Topical or intracameral administration of LAT-A reversibly and dose- and time-dependently increases outflow facility and lowers intraocular pressure in monkeys [10,11]. In cultured bovine aortic endothelial cells (BAEC), LAT-A induces reversible disruption of actin microfilaments, cell separation and cell loss [10]. However, the effects of LAT-A on the trabecular meshwork and Schlemm's canal (SC), its ocular target tissues for increasing outflow facility, have not been defined. To understand the cellular/molecular basis by which LAT-A affects outflow facility in vivo, we determined the effect of LAT-A on the morphology, cytoskeleton, and cellular adhesions of HTM cells in culture.

## METHODS

**HTM cell culture and LAT-A treatment:** HTM cells established at University of California, San Francisco, were shipped

to Madison, WI on dry ice and stored in liquid nitrogen prior to plating. Cells were grown on glass cover slips pre-coated with poly-L-lysine (Sigma Chemical Co., St. Louis, MO), and maintained in Dulbecco's modified Eagle medium (DMEM) supplemented with 10% fetal bovine serum, 25  $\mu$ g/ml gentamycin and 2.5  $\mu$ g/ml amphotericin B, at 37°C, 8% CO<sub>2</sub>. Cells of third through fifth passage were used 1 week after reaching confluence, at which time they exhibited a stable endothelial-like morphology.

**Imaging:** For videographic analysis of cultured HTM cells, a high performance monochrome CCD camera (COHU Inc., San Diego, CA) was attached to the phototube of a microscope (objective: 200x; phase contrast; numerical aperture: 0.3 mm, and tube length: 160 mm, Leica, Wetzlar, Germany) and the output was fed to a video recorder and TV screen. Cells were recorded in time-lapse (1-2 min intervals) before and during exposure to LAT-A and after LAT-A withdrawal using phase contrast optics. For each dose, the identical field of cells was located and recorded at each time interval. Images were subsequently captured off the videotape and subjected to morphometric evaluation.

**Immunofluorescence microscopy:** Immunofluorescence labeling was performed as previously described in detail [1,4,10]. Briefly, cells were washed with 50 mM MES (2-(N-morpholine) ethanesulfonic acid) buffer, permeabilized and fixed with 0.5% Triton X-100 and 3% paraformaldehyde in buffer. FITC-conjugated phalloidin (Sigma) was used for fluorescent labeling of actin. The primary antibodies used in this study were: monoclonal anti-human vinculin (clone hVin-1; Sigma), anti- $\beta$ -catenin (clone 15B8; Sigma) and anti-paxillin (clone 349, Transduction Laboratories, Lexington, KY), and

Correspondence to: Paul L. Kaufman, Department of Ophthalmology and Visual Sciences, F4/328 CSC, 600 Highland Ave., Madison, WI 53792-3220; Phone: (608) 263-6074; FAX: (608) 263-1466; email: [kaufmanp@mhuh.opth.wisc.edu](mailto:kaufmanp@mhuh.opth.wisc.edu)

rabbit anti-phosphotyrosine (Transduction Laboratories). Secondary antibodies (all from Jackson ImmunoResearch Laboratories, West Grove, PA, unless otherwise indicated) were rhodamine (TRITC)-conjugated goat anti-mouse IgG H+L, CY3-conjugated goat anti-mouse IgG H+L, and Alexa 488 conjugated goat anti-rabbit IgG H+L (Molecular Probes, Inc., Eugene, Oregon).

**Fluorescence ratio imaging (FRI):** To gain insight into the earliest changes in the molecular composition of cell-ECM and cell-cell adhesions in HTM cells treated with LAT-A, digital microscopy was employed. Images were acquired using the DeltaVision system (Applied Precision, Issaquah, WA), equipped with a Zeiss Axiovert 100 microscope (Oberkochen, Germany), 100x 1.3 NA Plan-Neofluar objective (Zeiss) and Photometrics 300 series scientific-grade cooled camera (Tucson, AZ) reading 12 bit images. For quantitative processing, images were acquired and corrected. Two-color superpositioning of images, color spectrum presentation of fluorescence intensity, and FRI between two different com-

ponents using double-labeled cells were performed, as previously described [12].

## RESULTS

**Effect of LAT-A on HTM cell morphology:** Cultured HTM cells form a confluent and flat monolayer with extensive intercellular contacts. Cells were recorded in time-lapse (1-2 min intervals) before and during exposure to 0.02, 0.2 and 2  $\mu$ M LAT-A. After 24 h exposure to LAT-A at each dose, recovery was evaluated by culturing the cells in LAT-A-free medium for another 24 and 48 h. HTM cell morphology appeared to change systematically with increasing LAT-A concentrations and incubation time. At 6 h after exposure to 2  $\mu$ M LAT-A, cells appeared obviously retracted and rounded, and became more markedly rounded but still remained attached at 24 h (Figure 1). At 0.2  $\mu$ M LAT-A, the effect was milder and cells mildly rounded up after 24 h of treatment (Figure 1). The lowest concentration of LAT-A used here (0.02  $\mu$ M) had no obvious effect on cell morphology up to 24 h. Recovery at all

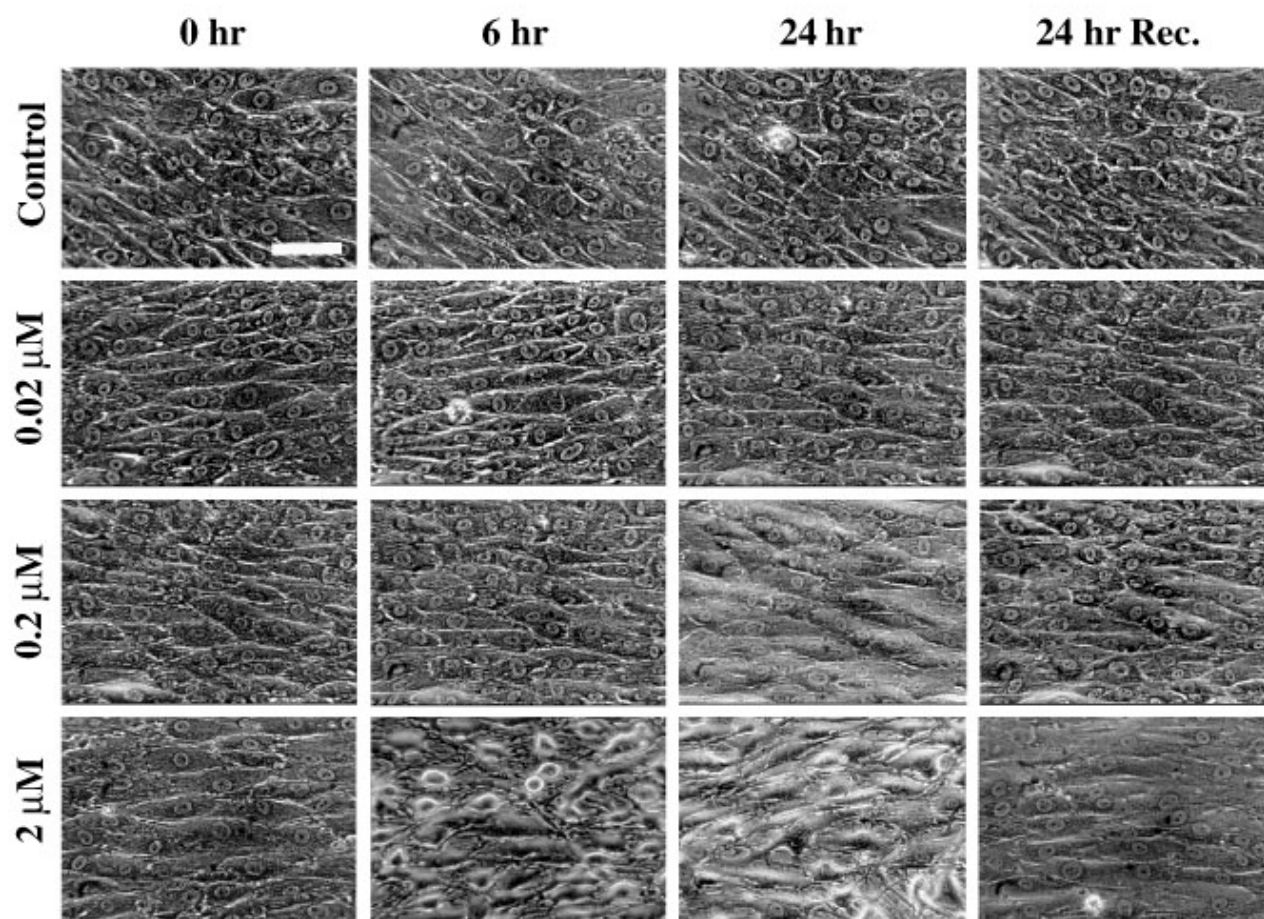


Figure 1. Effect of LAT-A on HTM cell morphology over time. Videographic recording of HTM cell morphology after treatment with 0, 0.02, 0.2 and 2  $\mu$ M LAT-A for 0, 6, and 24 h, and recovery for another 24 h. For each dose, the same field of cells was recorded at each time point. At 1, 6, 11, and 24 h at 0.02  $\mu$ M LAT-A, cell morphology appeared unchanged. At 0.2  $\mu$ M LAT-A, cells appeared slightly rounded at 24 h. At 2  $\mu$ M LAT-A, cells showed time-dependent morphological changes including cell rounding and separation. Recovery at all doses seemed almost complete after 24 and 48 h in LAT-A-free medium. Data for 1 and 11 h treatment and 48 h recovery are not shown. Bar = 80  $\mu$ m.



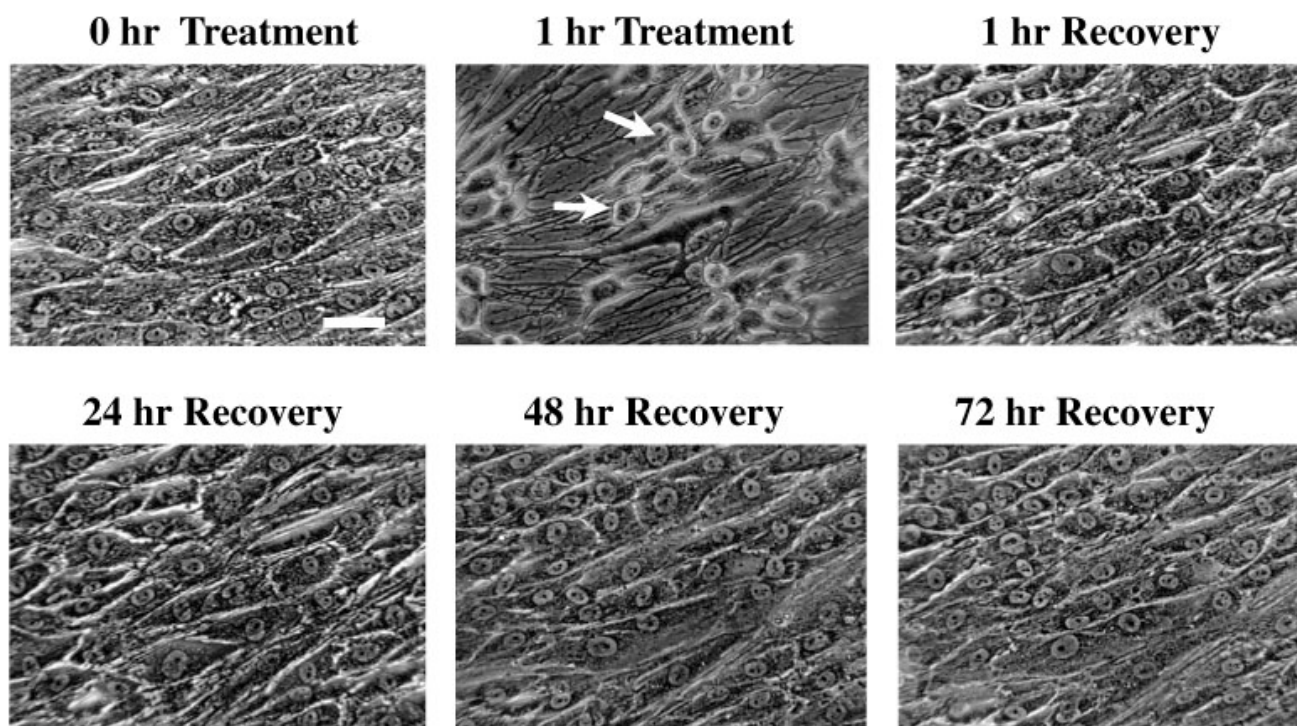


Figure 2. Recovery of HTM cell morphology from effect of high dose LAT-A treatment over time. Videographic recording of the recovery of HTM cell morphology following incubations for 1, 24, 48 and 72 h in LAT-A-free medium after treatment with 10  $\mu$ M LAT-A for 1 h. The LAT-A-treated cells initially lost their normal morphology and some appeared markedly retracted (arrows). Within 1 h, dramatic recovery of cell morphology occurred, and within 48 h recovery was essentially complete. Bar = 80  $\mu$ m.

doses seemed almost complete after 24 h in LAT-A-free medium, manifested by a full complement of cells appearing flattened, packed and virtually identical to 0-hour cells (Figure 1).

To determine recovery of cells exposed to a high LAT-A dose for a relatively short time, HTM cells treated with 10  $\mu$ M LAT-A (twice the highest in vivo intraocular concentration studied [10]) were recorded after 1 h of treatment and following 1, 24, 48, and 72 h of recovery. Cells treated with 10  $\mu$ M LAT-A displayed dramatic morphological changes within 1 h, appearing highly retracted and disorganized. However, no detached cells were observed, and major recovery was apparent after 1 h in LAT-A-free medium, and seemed almost complete by 48 h (Figure 2).

**Effect of LAT-A on actin filaments and cellular adhesions:** In untreated cells, fluorescent staining for F-actin showed numerous thick stress fibers oriented primarily parallel to the long axes of the confluent cells (Figure 3A). Vinculin was associated with both focal adhesions and cell-cell junctions (Figure 3B), and located at the termini of the actin bundles (Figure 3A,B). The cell-cell adhesions delineated by  $\beta$ -catenin staining appeared as continuous or partially segmented lines along the borders of the tightly packed cells (Figure 3C).

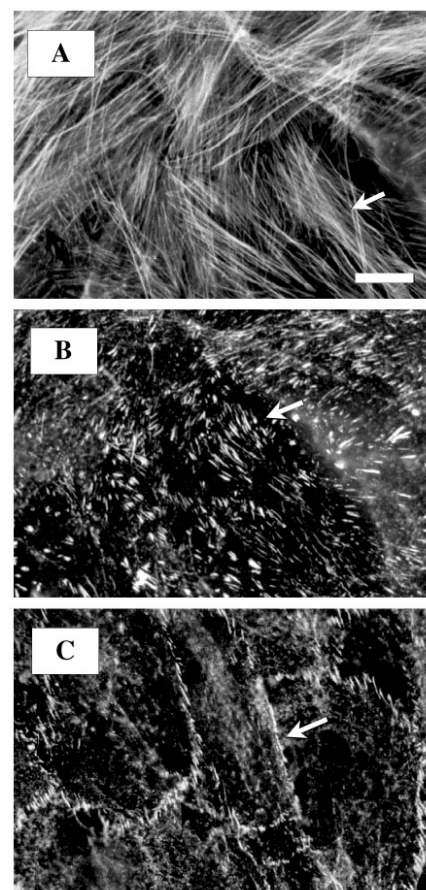


Figure 3. Distribution and organization of actin filaments and actin-related proteins in normal HTM cells. Fluorescent staining for actin revealed numerous stress fibers oriented primarily parallel to the long axis of the cells (A) and terminating at vinculin-containing focal adhesions and adherens junctions (A, B). Panels A and B are the same cells. Intercellular junctions were delineated by  $\beta$ -catenin staining appearing as continuous or partially segmented lines at cell-cell borders (C). The arrows point to actin stress fibers (A), vinculin-containing focal adhesions (B), and  $\beta$ -catenin containing cell-cell junctions (C). Bar = 30  $\mu$ m.



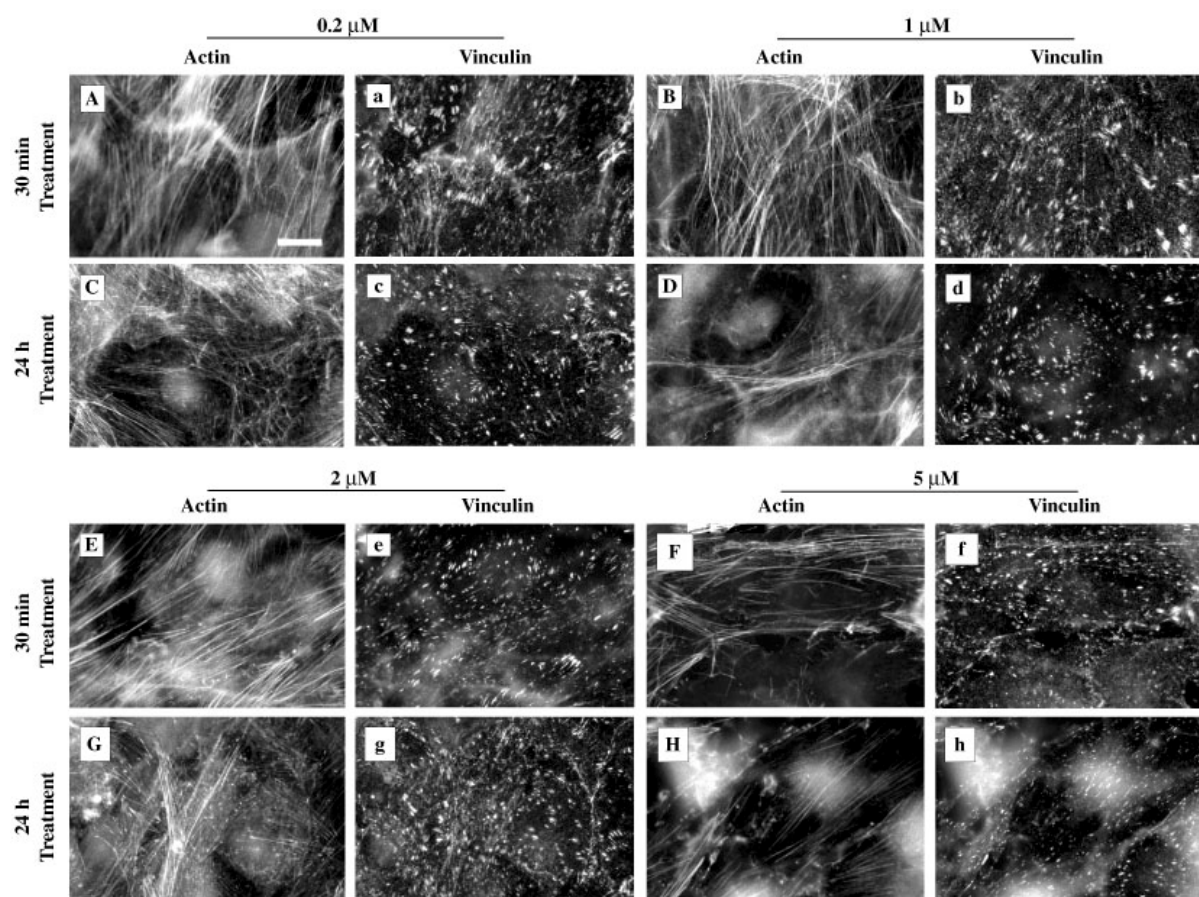


Figure 4. Effect of LAT-A on the distribution of actin and vinculin in cultured HTM cells. Effect of LAT-A on the distribution of actin and vinculin in cultured HTM cells treated with 0.2, 1, 2, or 5  $\mu$ M LAT-A for 30 min and 24 h, and double-labeled for actin (panels **A-H**) and vinculin (panels **a-h**). See Figure 3A and Figure 3B for normal actin and vinculin distribution and Figure 6 for actin and vinculin distribution after LAT-A treatment for 2 h. LAT-A resulted in progressive deterioration of actin filaments, and time- and dose-dependent disorganization of vinculin-containing focal contacts. The latter appeared more resistant to LAT-A than the  $\beta$ -catenin-containing intercellular adhesions, even at higher doses and longer treatment duration (panels **g** and **h**; compare with Figure 5). Bar = 20  $\mu$ m.

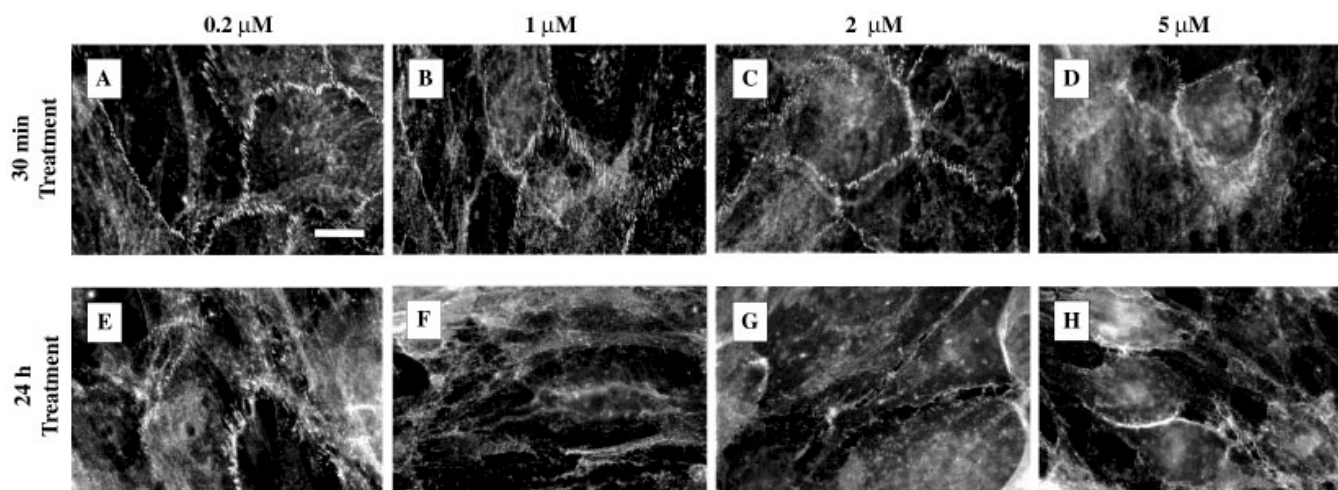


Figure 5. Effect of LAT-A on the distribution of  $\beta$ -catenin in HTM cells. Effect of 0.2, 1, 2, or 5  $\mu$ M LAT-A for 30 min and 24 h on the distribution of  $\beta$ -catenin in cultured HTM cells. See Figure 3C for normal  $\beta$ -catenin distribution, and Figure 7 for  $\beta$ -catenin distribution after 2 h LAT-A treatment. LAT-A induced time- and dose-dependent disorganization and disruption of  $\beta$ -catenin-containing intercellular junctions.  $\beta$ -catenin staining appeared to be affected as early as 30 min after 1  $\mu$ M LAT-A treatment. Within 24 h at the lowest LAT-A dose (0.2  $\mu$ M), staining at cell-cell borders became irregular and often discontinuous (panel **E**). At higher doses, most cell-cell borders completely disappeared and some cells separated (panels **F-H**). Bar = 20  $\mu$ m.



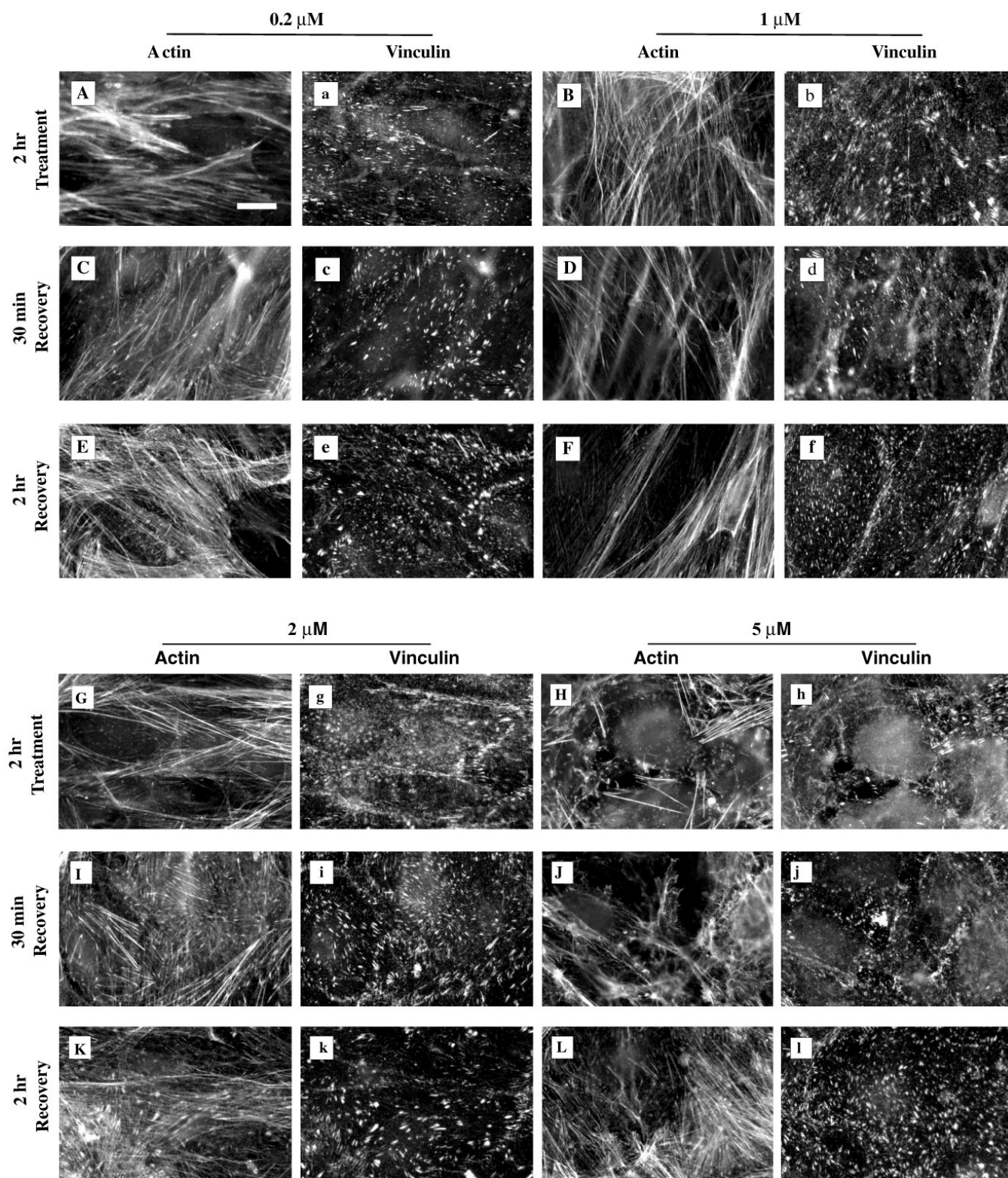


Figure 6. Actin and vinculin recovery in HTM cells after LAT-A treatment. Recovery of actin-based and vinculin-containing focal adhesions in cultured HTM cells after treatment with 0.2, 1, 2, or 5  $\mu$ M LAT-A for 2 h, and recovery for 30 min or 2 h in LAT-A-free medium. Recovery of the actin-based cytoskeleton (panels C, D, I, and J) and vinculin-containing focal adhesions (panels c, d, i, and j) after 2 h exposure to LAT-A was apparent by 30 min. Recovery was more complete following treatment with lower doses of LAT-A and longer recovery times (panels E, F, e, and f). Bar = 20  $\mu$ m.

In HTM cells treated with doses of LAT-A ranging from 0.2  $\mu$ M to 5  $\mu$ M for 30 min, 2 h and 24 h, LAT-A induced a time- and dose-dependent disruption of the stress fiber network and focal adhesions. Actin bundles had deteriorated markedly after 30 min exposure to 1  $\mu$ M LAT-A, appearing thinner, shorter and curved (Figure 4B). With longer exposures (24 h) and higher LAT-A concentrations (2 and 5  $\mu$ M), the stress fiber network was almost totally obliterated, leaving residual diffuse actin filaments distributed mostly at the cell periphery (Figure 4G,H). LAT-A-treated cells also underwent dramatic dose- and time-dependent deterioration of  $\beta$ -catenin-containing cell-cell adhesions (Figure 5A-H). Disruption of adherens junctions was apparent already after 30 min of treatment with 1  $\mu$ M LAT-A, and the effect increased with incubation time and/or LAT-A concentration. Vinculin-rich focal contacts were reduced in size and number and appeared disorganized after LAT-A treatment, but, in general, they appeared more resistant to LAT-A treatment than cell-cell junctions (Figure 4 and Figure 5). After 1 or 2  $\mu$ M LAT-A treatment for 24 h, there were still significant amount of vinculin patches remaining, while  $\beta$ -catenin-containing cell-cell adhesions were almost completely disrupted or disappeared (Figure 4 and Figure 5).

**Recovery of actin, vinculin and  $\beta$ -catenin organization after LAT-A withdrawal:** For assessment of recovery of cytoskeletal and junctional structures, cells were treated with LAT-A for 2 h, after which medium was changed to LAT-A-free medium for 30 min and 2 h. Recovery of the actin-based cytoskeleton, vinculin-containing focal adhesions, and  $\beta$ -catenin-containing cell-cell adherens junctions after 2-h treat-

ment with 0.2 and 1  $\mu$ M LAT-A was apparent as early as 30 min after drug withdrawal. The recovery was, however, more complete and faster at lower doses of LAT-A than at 2 and 5  $\mu$ M. Actin and vinculin recovered most rapidly, redistributing in both radial and circumferential patterns. Vinculin patches were again located at the termini of the actin bundles and increased in size, number, and density when the actin bundles became thick and dense (Figure 6).  $\beta$ -catenin showed partial recovery within 30 min, displaying a punctate or zigzag pattern along cell-cell contacts, but recovery seemed slower compared to that of actin and vinculin (Figure 7).

**FRI analysis of LAT-A induced changes in the actin cytoskeleton and the associated focal contact and adherens junction proteins:** Standard immunofluorescence analysis of HTM cells treated with various LAT-A concentrations demonstrated that there was a striking, yet reversible, breakdown in the structure and organization of actin, vinculin and  $\beta$ -catenin. A recently described technique, fluorescence ratio imaging (FRI, [12]), was utilized in order to examine the molecular dynamics of these changes in more detail. Cells were double-labeled for vinculin and actin, paxillin and phosphotyrosine, or  $\beta$ -catenin and actin, before or after 0, 15, or 60 min exposure to 0.2-5  $\mu$ M LAT-A. Cells treated with LAT-A for 1 h and then incubated in LAT-A-free medium for 5 or 20 min were also double-labeled as above.

Double labeling of HTM cells for vinculin (red channel) and actin (green channel) in untreated cells (Figure 8A-D) confirmed the earlier results showing well-organized actin filaments terminating in vinculin-positive focal adhesions. FRI

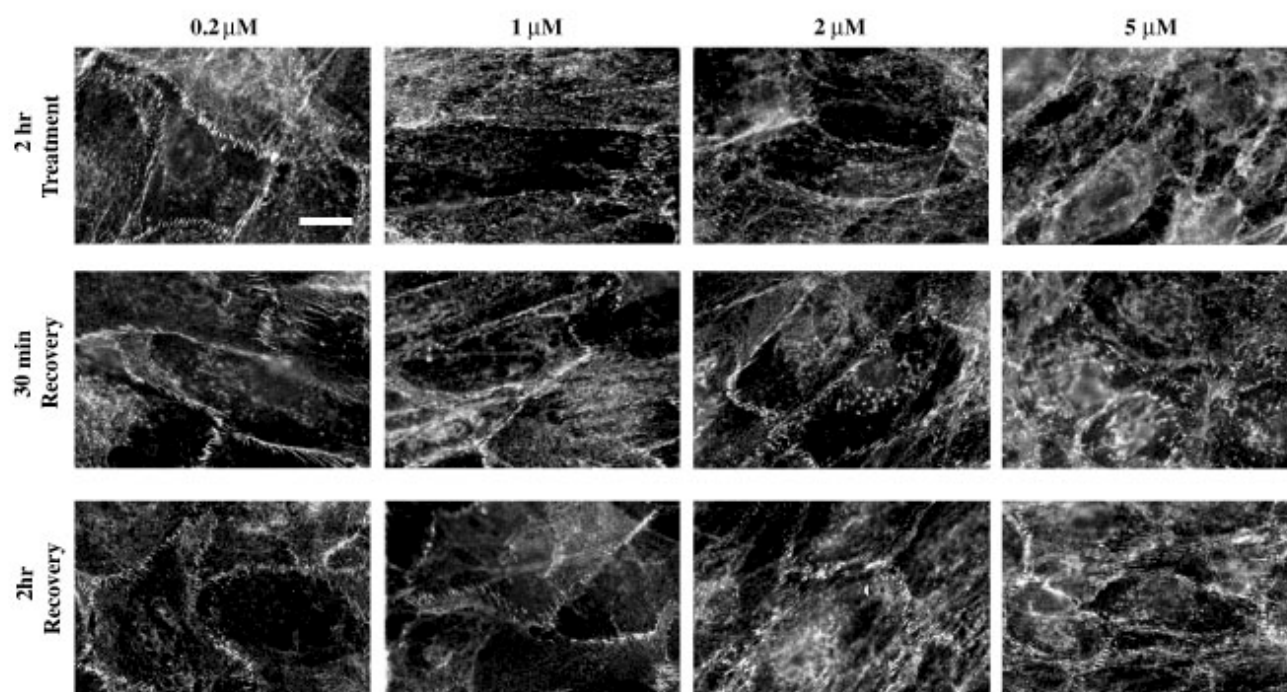


Figure 7.  $\beta$ -catenin recovery in HTM cells after LAT-A treatment. Recovery of  $\beta$ -catenin-containing intercellular adhesions in cultured HTM cells after treatment with 0.2, 1, 2, or 5  $\mu$ M LAT-A for 2 h, and recovery for 30 min and 2 h in LAT-A-free medium.  $\beta$ -catenin recovery was slow and incomplete, compared to that of actin and vinculin following similar treatments (compare with Figure 6). Bar = 20  $\mu$ m.



analysis (Figure 8D) showed that within most individual adhesions, there was extensive overlap between vinculin and actin labeling (i.e., abundance of sites where a 1:1 intensity ratio was apparent). After exposure to LAT-A for as little as 15 min (Figure 8E-H), there was a breakdown of actin stress fibers and a reduction in the number and size of vinculin-positive adhesions. FRI indicated that the actin:vinculin ratio within the vast majority of residual adhesions dropped dramatically to below 0.1, indicating a relative

loss of actin from these structures (Figure 8H). The vinculin-positive focal contact-like structures did not completely disappear even after 1 h of exposure to 1  $\mu$ M LAT-A (Figure 8I-L), which is consistent with findings with other cell types showing some resistance of focal adhesions to low concentrations of LAT-A [10]. Those that do remain contained vinculin and actin in a 1:1 ratio (Figure 8L). Examination of absolute fluorescent labeling intensities within the latter sites found a decrease in vinculin-positive staining rather than an increase in actin-positive staining at the 1 h LAT-A exposure time point compared to the 15 min exposure time point. Together, the data indicate a rapid loss of actin filaments from focal adhesions followed by a slower loss of vinculin upon exposure to LAT-A. Removal of the drug for as little as 5 min resulted in a rapid reorganization of actin filaments and increase in the size, number, and intensity of vinculin-positive focal adhesions, although it appeared that filamentous actin recovery was more advanced than the focal adhesion recovery (Figure 8M-P). By 20 min after LAT-A removal, actin and vinculin appeared essentially as in untreated cells (Figure 8Q-T).

Double labeling of HTM cells for actin (green channel) and  $\beta$ -catenin (red channel; Figure 9) again

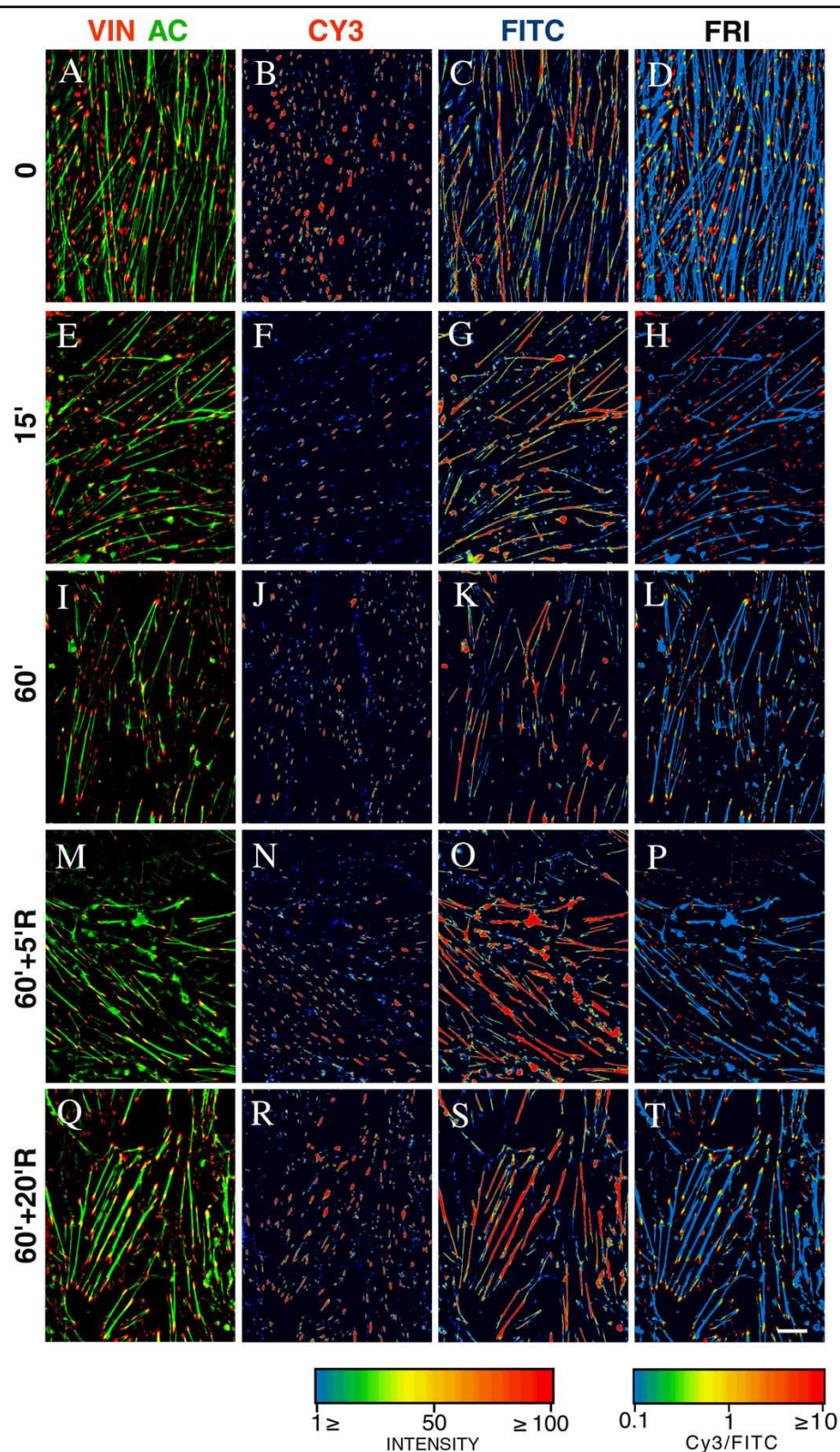


Figure 8. FRI of vinculin and actin in HTM cells treated with LAT-A. Panels A-L: Digital microscopic analysis of HTM cells, double-labeled for vinculin (VIN; CY3) and actin (AC; FITC), before (0) and after 15 and 60 min treatment (15', 60') with 1  $\mu$ M LAT-A. Panels M-T: Cells treated with LAT-A for 1 h and then incubated in medium without LAT-A for 5 or 20 min (60'+5'R; 60'+20'R). The left column shows the superimposed images of vinculin (red) and actin (green). The columns marked CY3 and FITC show the intensity of labeling of the respective proteins, using the spectrum scale presented under the FITC column. The FRI column depicts the CY3-to-FITC intensity ratio (scale shown under the column). Bar = 10  $\mu$ m.



showed that cell-cell adhesions were also highly LAT-A sensitive, in line with earlier experiments conducted with other cell types [10,13]. FRI showed that in untreated cells little, if any, actin was associated with the sharp band of junctional  $\beta$ -catenin, evidenced by the high  $\beta$ -catenin:actin ratio within these structures (Figure 9D). Actin filaments were detected in the vicinity of the junctions flanking the  $\beta$ -catenin bands. Upon exposure to LAT-A for 15 min, the size and shape of the  $\beta$ -catenin containing sites were

dramatically altered (Figure 9E-H), but differently from vinculin, which was less sensitive to the drug (compare with Figure 8E-H). The  $\beta$ -catenin-positive adhesions decreased in number and tended to aggregate at cell-cell borders. FRI analysis showed that the residual actin filaments were not associated with these  $\beta$ -catenin containing adhesions (Figure 9H). By 60 min of LAT-A exposure (Figure 9I-L), most of the  $\beta$ -catenin aggregates, as well as many small punctate  $\beta$ -catenin-containing structures, appeared scattered throughout the cytoplasm and were no longer associated with cell-cell borders. Removal of LAT-A, again, resulted in a rapid reformation of actin filaments. However, in contrast to the response of vinculin-containing focal adhesions,  $\beta$ -catenin-positive structures remained disorganized and did not recover for up to 60 min after LAT-A removal (Figure 9M-T).

Finally, given the differential effects of LAT-A on actin, vinculin and  $\beta$ -catenin, HTM cells were double-labeled for paxillin (red channel) and phosphotyrosine (green channel; Figure 10A-T). Paxillin, unlike vinculin, was localized only to cell-matrix, but not to cell-cell adhesions in other cells, while phosphotyrosine could be localized in both types of adhesion [12,14]. Zamir et al. [12] found that fibro-

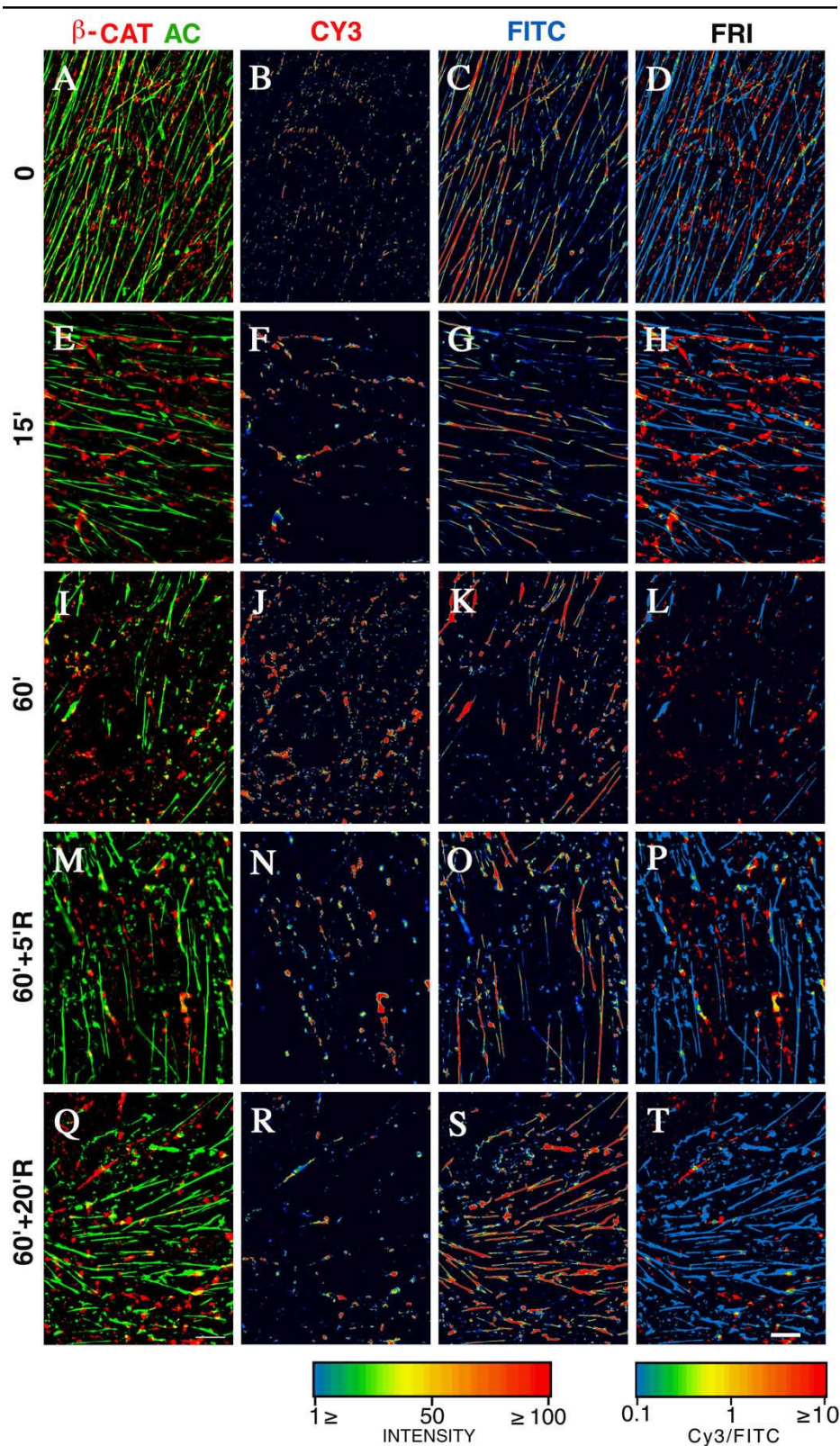


Figure 9. FRI of  $\beta$ -catenin and actin in HTM cells treated with LAT-A. Panels A-L: Digital microscopic analysis of HTM cells, double-labeled for  $\beta$ -catenin ( $\beta$ -CAT; CY3) and F-actin (AC; FITC), before (0) and after 15 and 60 min treatment (15', 60') with 1  $\mu$ M LAT-A, or panels M-T treated with LAT-A for 1 h and then incubated in medium without LAT-A for 5 or 20 min (60'+5'R; 60'+20'R). The left column shows the superimposed images of  $\beta$ -catenin (red) and F-actin (green). The columns marked CY3 and FITC show the intensity of labeling of the respective proteins using the spectrum scale presented under the FITC column. The FRI column depicts the CY3-to-FITC intensity ratio (scale shown under the column). Bar = 10  $\mu$ m.



blasts treated with the kinase inhibitor H-7, which blocks actomyosin contractility, display disrupted phosphotyrosine-, paxillin-, and vinculin-containing cell-matrix adhesions [12]. In untreated HTM cells (Figure 10A-D), paxillin and phosphotyrosine demonstrated extensive co-localization within focal adhesions, manifested by the abundance of adhesions with a 1:1 intensity ratio. LAT-A treatment for 15 or 60 min decreased the intensity, but apparently not the number of phosphotyrosine-positive sites (compare Fig-

ure 10C with Figure 10G and Figure 10J). In contrast, there was a significant reduction in the number and intensity of paxillin-positive adhesions (compare Figure 10B with Figure 10F and Figure 10I) and within many of the latter, the ratio of paxillin to phosphotyrosine was high (Figure 10H). These data indicated a selective loss of phosphotyrosine followed by paxillin from focal adhesions upon exposure to LAT-A. Shortly (5 min) after removal of LAT-A, there was limited re-appearance of paxillin or phosphotyrosine in focal adhesions (compare Figure 10N and Figure 10O with Figure 10J and Figure 10K, respectively), compared to vinculin (compare with corresponding panels in Figure 8). By 20 min the number and intensity of paxillin-positive sites increased and were similar to that of untreated cells. Likewise, the number and intensity of phosphotyrosine-positive sites increased at this time point, but FRI showed that there was still relatively little phosphotyrosine associated with the paxillin-positive sites (Figure 10Q-T). This suggests that tyrosine phosphorylation within individual focal adhesions was more sensitive to the effects of LAT-A than was the actual assembly of proteins into those adhesions.

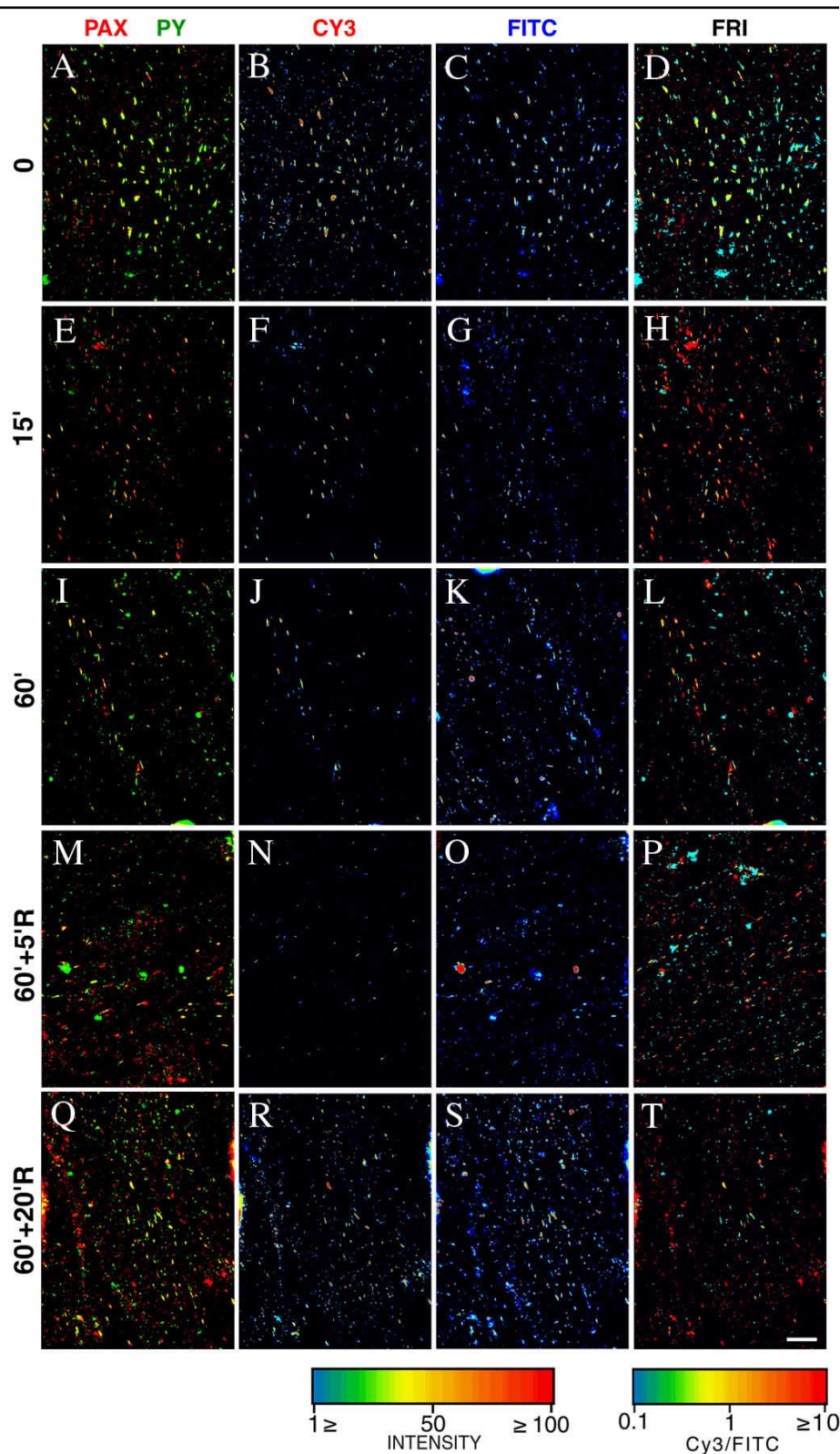


Figure 10. FRI of paxillin and phosphotyrosine in HTM cells treated with LAT-A. Panels A-L: Digital microscopic analysis of HTM cells, double-labeled for paxillin (PAX; CY3) and phosphotyrosine (PY; FITC), before (0) and after 15 and 60 min treatment (15', 60') with 1  $\mu$ M LAT-A. Panels M-T: cells treated with LAT-A for 1 h and then incubated in medium without LAT-A for 5 or 20 min (60'+5'R; 60'+20'R). The left column shows the superimposed images of paxillin (red) and phosphotyrosine (green). The columns marked CY3 and FITC show the intensity of the respective labeling, using the spectrum scale presented under the FITC column. The FRI column depicts the CY3-to-FITC intensity ratio (scale shown under the column). Bar = 10  $\mu$ m.

## DISCUSSION

Actin filaments and actin-associated proteins play an important role in cell-substratum and cell-cell interaction, extracellular signal transduction, cytoskeleton organization and cell morphology and contractility [15,16]. Actin filaments interact closely with the plasma membrane at the cytoplasmic face of cell-cell and cell-ECM adhesions [17,18]. With LAT-A treatment, HTM cells retract time- and dose-dependently, as evidenced by “rounding” or “thickening”, indicating a perturbation of cellular anchorage and overall architecture. This is attributable to the capacity of LAT-A to disrupt the actin cytoskeleton, leading to deterioration of microfilament bundles, loosening of cell-cell attachments, and cell retraction. With high dose and long duration exposure to LAT-A, stress fiber organization was almost completely disrupted, leading to the cell retraction and rounding up observed by phase contrast. Indeed, the changes in the actin filaments and cellular adhesions of cells treated with 0.2 or 2  $\mu$ M LAT-A for 24 h (Figure 3, Figure 4, and Figure 5) corresponded well with the changes in cell morphology at the same drug concentrations and treatment time (Figure 1).

LAT-A sequesters monomeric actin, thereby inhibiting actin assembly and disrupting the actin cytoskeleton [8,19]. Consequently, this drug disrupts the actin-dependent intercellular (adherens) junctions and cell-matrix (focal) adhesions [11]. H-7 and other kinase inhibitors affecting myosin II-dependent contractility disrupt the stress fiber network and destroy focal contacts without disrupting cell-cell interactions. Thus, while both drugs could affect flow dynamics via a common mechanism (namely loss of cellular contractility of trabecular cells), LAT-A, via its unique effect on adherens junctions, might also form new intercellular flow pathways.

It is noteworthy that the kinetics of LAT-A's effect on stress fibers and on vinculin-containing focal contacts were quite different. Actin filaments were rapidly lost upon treatment of HTM cells with LAT-A, and the recovery of actin after LAT-A withdrawal was also rapid (within 5 min). Significant disappearance and reappearance of vinculin-containing focal contacts, on the other hand, was relatively slow (within 60 min and 20 min, respectively). These differences may stem from LAT-A affecting actin primarily, with disruption of focal contacts following secondarily. Vinculin is an important component of a protein complex that links the actin network to the plasma membrane at adhesion sites [20], and its expression is affected by the level of actin expression [21], suggesting that vinculin may serve as a cytoskeletal protein functioning downstream from actin in forming cellular adhesions. As a structural protein in membrane-cytoskeleton interactions, vinculin loses its normal distribution and organization as a result of actin disruption upon LAT-A treatment. Therefore, actin recovery will be followed by vinculin recovery that links the actin cytoskeleton to the cell membrane for reformation of focal contacts.

This is consistent with *in vitro* and *in vivo* studies regarding the effects of cytoskeleton active agents on outflow facility [3-6,10,11]. The sequence of events underlying the rapid effects of LAT-A and H-7 on outflow facility is not entirely

clear and may differ. TM cells, like other endothelial cells [22], normally maintain an active contractile tone. LAT-A, which directly binds to G-actin, disrupts the actin microfilament network and consequently interferes with cell contractility and adhesion [23]. In contrast, H-7, a myosin light chain kinase inhibitor, suppresses actomyosin-driven contractility primarily, leading secondarily to deterioration of the actin microfilament system [1]. Cellular contractility, rather than actin filament disruption, plays a primary role in assembly/disassembly of focal contacts [12,24]. H-7 may exert its outflow facility increasing effects primarily by promoting TM cell relaxation, with secondary actin filament degradation being physiologically less relevant. The opposite sequence may occur with LAT-A, and we cannot be sure which event (cellular relaxation or actin filament degradation) matters most for facility.

Trabecular cells on the corneoscleral trabecular beams and in the juxtacanalicular tissue play a critical role in overall meshwork architecture and the conductance of aqueous humor. TM cells are involved in the secretion and metabolism of the complex ECM, and provide an endothelial-like lining for the entire pathway [25]. The extensive microfilament-associated molecular interactions or “cross-talk” between TM cells, and between cells and their underlying ECM, likely contribute to the control of outflow resistance. These interactions represent a point at which pharmacological control of intraocular pressure may be possible. LAT-A exerts a significant facility-increasing effect, at least in part by mechanisms related to perturbations in the cytoskeleton, the ECM, or their interactions. The facility increase in monkeys is reversible within 3 h after drug removal [10], consistent with the reversibility of LAT-A's effects on cultured HTM cells. Nearly full recovery from a severe change in cell shape induced by 1-h exposure to 10  $\mu$ M LAT-A (twice the maximal facility-effective dose) occurred within 1 h in drug-free medium, with no cell loss, indicating that the cells remained viable. LAT-A may thus induce a physiological modulation of a basic control mechanism rather than irreversible toxicity, auguring well for possible clinical applicability if targeted specifically to cells of the conventional outflow pathway. The large increases in outflow facility achieved with other cytoskeletal active agents, including cytochalasins B and D [5,6] and H-7 [4], are also reversible, again suggesting that the facility effects of these agents are closely associated with actin filament deterioration and recovery. Nonetheless, more specific studies of cell viability should be undertaken.

Topically or intracamerally administered latrunculin-B (LAT-B), another member of the latrunculin family which also inhibits actin assembly, also dose- and time-dependently increases outflow facility in living monkeys [26]. In addition to lowering IOP consequent to the facility increase [11], both LAT-A and LAT-B increase protein concentration in the anterior chamber, induce cell shape changes and increased permeability in the corneal endothelium, and induce overall corneal thickening. These effects are relatively mild and completely reversible within hours, and the outflow facility and biomicroscopic appearance of the eyes are subsequently normal, indicating the absence of long-term *in vivo* toxicity at



least after a single facility-effective dose [11]. Although LAT-B is more potent and effective than LAT-A at increasing facility, the other anterior segment changes are less pronounced following LAT-B than with LAT-A in the living monkey [11]. Epstein et al. [27] found that LAT-B increases outflow facility in organ cultured porcine eyes, and causes a substantial change in cell shape and attachments, associated with disruption of actin filaments but without effects on tubulin staining, in cultured HTM and Schlemm's canal cells. No apparent signs of cellular toxicity were found in the perfused porcine eyes by transmission electron microscopy [27], indicating that latrunculins may have strong but relatively "safe" effects on the cells of the ocular anterior segment [11]. Studies following longer-term dosing would be important in this regard. More work is needed on the assembly and disassembly of actin and actin-associated adhesion proteins of HTM cells treated with LAT-A and other agents, to optimize outflow facility enhancement without risking irreversible changes in the fine anatomy of the outflow pathway or other anterior segment tissues. Different drug administration strategies might also reduce the side effects. Administering lower concentrations of LAT-A over a longer time, aided by the pressure/flow gradient across the trabecular meshwork, might increase outflow facility and decrease IOP without affecting the cornea or ciliary body. High concentration/small volume formulations used in most experimental topical drug protocols and clinical therapy place the cornea at a disadvantage. Using lower concentrations in larger volumes to spread the drug more evenly over the entire corneal surface and expose the central cornea to a much lower dose, and the use of other vehicles, delivery systems and penetration routes that are less toxic to the cornea, could be explored.

### ACKNOWLEDGEMENTS

This work was supported by grants from the National Eye Institute (EY02698 to PLK, EY02477 to JRP); Research to Prevent Blindness (PLK); Glaucoma Research Foundation (PLK, JRP, BG); and Yeda Research and Development, the E. Neter Chair in Cell and Tumor Biology, the Minerva Foundation, and the Israel Science Foundation, Rehovot, Israel (BG). We thank Donald J. Fauss for technical assistance with HTM cell culture, and Mary Ann Croft for assistance with image analysis.

### REFERENCES

- Volberg T, Geiger B, Citi S, Bershadsky AD. Effect of protein kinase inhibitor H-7 on the contractility, integrity, and membrane anchorage of the microfilament system. *Cell Motil Cytoskeleton* 1994; 29:321-38.
- Birrell GB, Hedberg KK, Habliston DL, Griffith OH. Protein kinase C inhibitor H-7 alters the actin cytoskeleton of cultured cells. *J Cell Physiol* 1989; 141:74-84.
- Liu X, Glasser A, Croft MA, Polansky JR, Fauss DJ, Kaufman PL. Effect of H7 on cultured trabecular meshwork (HTM) cells. *Invest Ophthalmol Vis Sci* 1998; 39:S705.
- Tian B, Kaufman PL, Volberg T, Gabelt BT, Geiger B. H-7 disrupts the actin cytoskeleton and increases outflow facility. *Arch Ophthalmol* 1998; 116:633-43.
- Kaufman PL, Erickson KA. Cytochalasin B and D dose-outflow facility response relationships in the cynomolgus monkey. *Invest Ophthalmol Vis Sci* 1982; 23:646-50.
- Kaufman PL, Barany EH. Cytochalasin B reversibly increases outflow facility in the eye of the cynomolgus monkey. *Invest Ophthalmol Vis Sci* 1977; 16:47-53.
- Tripathi BJ, Tripathi RC. Effect of epinephrine in vitro on the morphology, phagocytosis, and mitotic activity of human trabecular endothelium. *Exp Eye Res* 1984; 39:731-44.
- Coue M, Brenner SL, Spector I, Korn ED. Inhibition of actin polymerization by latrunculin A. *FEBS Lett* 1987; 213:316-8.
- Spector I, Shochet NR, Blasberger D, Kashman Y. Latrunculins—novel marine macrolides that disrupt microfilament organization and affect cell growth: I. Comparison with cytochalasin D. *Cell Motil Cytoskeleton* 1989; 13:127-44.
- Peterson JA, Tian B, Bershadsky AD, Volberg T, Gangnon RE, Spector I, Geiger B, Kaufman PL. Latrunculin-A increases outflow facility in the monkey. *Invest Ophthalmol Vis Sci* 1999; 40:931-41.
- Peterson JA, Tian B, McLaren JW, Hubbard WC, Geiger B, Kaufman PL. Latrunculins' effects on intraocular pressure, aqueous humor flow, and corneal endothelium. *Invest Ophthalmol Vis Sci* 2000; 41:1749-58.
- Zamir E, Katz BZ, Aota S, Yamada KM, Geiger B, Kam Z. Molecular diversity of cell-matrix adhesions. *J Cell Sci* 1999; 165:55-69.
- Bershadsky AD, Gluck U, Denisenko ON, Sklyarova TV, Spector I, Ben-Ze'ev A. The state of actin assembly regulates actin and vinculin expression by a feedback loop. *J Cell Sci* 1995; 108:1183-93.
- Chenn A, Zhang YA, Chang BT, McConnell SK. Intrinsic polarity of mammalian neuroepithelial cells. *Mol Cell Neurosci* 1998; 11:183-93.
- Geiger B, Yehuda-Levenberg S, Bershadsky AD. Molecular interactions in the submembrane plaque of cell-cell and cell-matrix adhesions. *Acta Anat* 1995; 154:46-62.
- Borowsky ML, Hynes RO. Layilin, a novel talin-binding transmembrane protein homologous with C-type lectins, is localized in membrane ruffles. *J Cell Biol* 1998; 143:429-42.
- Berezin V, Skladchikova G, Bock E. Evaluation of cell morphology by video recording and computer-assisted image analysis. *Cytometry* 1997; 27:106-16.
- Jockusch BM, Bubeck P, Giehl K, Kroemker M, Moschner J, Rothkegel M, Rudiger M, Schluter K, Stanke G, Winkler J. The molecular architecture of focal adhesions. *Annu Rev Cell Dev Biol* 1995; 11:379-416.
- Ayscough KR, Stryker J, Pokala N, Sanders M, Crews P, Drubin DG. High rates of actin filament turnover in budding yeast and roles for actin in establishment and maintenance of cell polarity revealed using the actin inhibitor latrunculin-A. *J Cell Biol* 1997; 137:399-416.
- Rudiger M. Vinculin and alpha-catenin: shared and unique functions in adherens junctions. *Bioessays* 1998; 20:733-40.
- Schevzov G, Lloyd C, Gunning P. Impact of altered actin gene expression on vinculin, talin, cell spreading, and motility. *DNA Cell Biol* 1995; 14:689-700.
- Doukas J, Cutler AH, Boswell CA, Joris I, Maino G. Reversible endothelial cell relaxation induced by oxygen and glucose deprivation. A model of ischemia in vitro. *Am J Pathol* 1994; 145:211-9.
- Peterson JA, Tian B, Geiger B, Kaufman PL. Latrunculin-A causes mydriasis and cycloplegia in the cynomolgus monkey. *Invest Ophthalmol Vis Sci* 1999; 40:631-8.

24. Helfman DM, Levy ET, Berthier C, Shtutman M, Rivelino D, Grosheva I, Lachish-Zalait A, Elbaum M, Bershadsky AD. Caldesmon inhibits nonmuscle cell contractility and interferes with the formation of focal adhesions. *Mol Biol Cell* 1999; 10:3097-112.
25. Polansky JR, Alvarado JA. Cellular mechanisms influencing the aqueous humor outflow pathway. In: Albert DM, Jakobiec FA, editors. *Principles and practice of ophthalmology: basic science*. Philadelphia: W. B. Saunders Co.; 1994. p. 226-251.
26. Peterson JA, Tian B, Geiger B, Kaufman PL. Effect of latrunculin-B on outflow facility in monkeys. *Exp Eye Res* 2000; 70:307-13.
27. Epstein DL, Rowlette L, Roberts BC. Acto-myosin drug effects and aqueous outflow function. *Invest Ophthalmol Vis Sci* 1999; 40:74-81.

The typographical corrections below were made to the article on the date noted. These changes have been incorporated in the article and the details are documented here.

18 August 2000:

In Figure 8, in the first sentence of the caption:

...before 0 and after 15 and 60 min treatment (15', 60') with 1  $\mu$ M LAT-A.

was changed to:

...before (0) and after 15 and 60 min treatment (15', 60') with 1  $\mu$ M LAT-A.

In Figure 9, in the first sentence of the caption:

...before (0) and after 15 and 60 min treatment (15', 60') with LAT-A,....

was changed to:

...before (0) and after 15 and 60 min treatment (15', 60') with 1  $\mu$ M LAT-A,....

In Figure 10, in the first sentence of the caption:

...before (0) and after 15 and 60 min treatment (15', 60') with LAT-A.

was changed to:

...before (0) and after 15 and 60 min treatment (15', 60') with 1  $\mu$ M LAT-A.